

Attenuated Total Reflectance (ATR) Study of Polymer Blend Films

R. POPLI and ANIL M. DWIVEDI, *Louis Laboratory, S. C. Johnson and Son, Inc., Racine, Wisconsin 53403*

Synopsis

Variable angle ATR was used to obtain a compositional depth profile of films cast from the blend solutions. Blend solutions were prepared from a colloid of high molecular weight styrene-acrylate-methacrylic acid copolymer, an alkali-soluble styrene-acrylic acid resin neutralized with ammonia and a colloid of copolymer of propylene. Films obtained from drying the blend solutions show a nonhomogeneous distribution of three polymers through the film thickness. This inhomogeneity cannot be explained solely on the basis of sedimentation effects due to density differences between three polymers. Experimental results of ATR using germanium and KRS-5 crystals are compared to provide estimates of the distance over which nonhomogeneous composition occurs.

INTRODUCTION

Attenuated total reflectance (ATR) is often described as a technique to examine the surface of materials, such as thin films or opaque solids.¹⁻³ In a typical ATR experiment, an evanescent IR beam penetrates into the specimen to a depth of the order of 1 μm . This thickness is 2-3 orders of magnitude greater than that examined by other surface characterization techniques such as ESCA, Auger, or SIMS. Therefore, ATR is not a surface characterization technique in a true sense. Nevertheless, it provides information on film compositions in a dimension scale not easily attained by other methods.^{4,5}

An important application of ATR is the study of a specimen at various angles of beam incidence. Changes in penetration depth of the evanescent beam with incidence angle allows measurement of composition at various depths inside the film. This application of ATR has generally been limited to a qualitative comparison of spectra for various incidence angles to show trends in film composition through its thickness. In recent years, theoretical and experimental studies have been carried out to advance the technique for quantitative measurement.⁶⁻⁹

In a study of polymer blends using ATR, one encounters additional difficulties due to overlap of bands from various components. Therefore, availability and selection of bands is extremely critical for obtaining reliable results.

In the present study, we examined ATR spectra of three-component blend films at various incidence angles. The results on concentration of components through the film thickness show a nonhomogeneous distribution of the three polymers near the film surface. Thermal measurements also suggest a phase-segregated film morphology.

TABLE I
 Characteristics of Polymers and Blends Used

Specimen	Polymer		Mol wt	Blend film composition (%)				Fluorosurfactant FSE
	Type	Composition		Polymer A	Polymer B	Polymer C	Fluorosurfactant FSE	
Polymer A	Emulsion	S/AMS/MMA/BA/MAA	$\bar{M}_n = 9100$ $\bar{M}_w = 125,260$	—	—	—	—	
Polymer B	Resin solution neutralized in ammonia/water	S/AMS/AA	$\bar{M}_n = 2400$ $\bar{M}_w = 5970$	—	—	—	—	
Polymer C	Emulsion	PP copolymer E-43 (Tennessee Eastman)	Few thousands	—	—	—	—	
B1	Blend	—		62.2	37.3	—	0.5	
B2	Blend	—		55.9	33.6	10.0	0.5	
B3	Blend	—		50.9	30.6	18.2	0.4	
B4	Blend	—		46.6	28.0	25.0	0.4	
B5	Blend	—		43.0	25.9	30.8	0.4	
B6	Blend	—		39.0	23.5	37.2	0.3	

EXPERIMENTAL

Three polymers comprising the blend in this study are: a styrene-acrylate-acrylic acid copolymer emulsion (polymer A), a styrene-methacrylic acid copolymer solution in ammonia/water (polymer B), and an emulsified polypropylene copolymer (polymer C). Polypropylene copolymer was received from Tennessee Eastman. Polymers A and B were synthesized and an emulsion of polypropylene copolymer was prepared at S. C. Johnson and Son, Inc. The ratio of ammonia to acid groups present in polymer B corresponds to a degree of neutralization of approximately 110%. These polymers are described in detail in Table I. A blend was prepared by mixing emulsion polymer A, a solution of polymer B, and deionized water in a beaker with constant stirring of the solution. Nonvolatile content of this mixture is approximately 17%. Solution blends of compositions shown in Table I were obtained by mixing a predetermined amount of emulsion polymer C with the blend of polymers A and B described above.

Aluminum foil was spread over a clean, smooth surface and was the substrate for casting films. ATR spectra of the aluminum foil showed no active band in the wavenumber region from 4000 to 600 cm^{-1} . A predetermined amount of the blend solution was spread over the substrate with a film drawing rod #12. Expected wet film thickness using this rod is 30.8 μm . After 2 h of drying, a second coat was applied in a similar manner. Films were dried at 72°F and 55% RH for at least a week. Dry film thickness is approximately 12 μm . Considering the nonvolatile content of the blends, dry film thickness is near the thickness expected from a 61.6 μm thick wet film.

ATR spectra were recorded on a Nicolet 60 SX FTIR Spectrometer using a germanium crystal. Strips of supported film $5 \times 1 \text{ cm}^2$ were placed inside ATR cell on each side of the crystal so that film surface was in contact with the crystal face. Incidence angles of 35°, 40°, 45°, and 50° were used for recording the spectra. The depth of penetration of IR beam (distance at which the evanescent beam intensity drops to 33% of its incident value) in the film is estimated at 0.55–0.30 μm using the germanium crystal.

Differential scanning calorimetry (DSC) of the blend films was done on a DuPont 910 DSC module/9900 thermal analyzer using nitrogen gas purge at a heating rate of 20°C/min. Indium and high-purity water were used to correct for instrument temperature offset. Sample sizes were 1 to 3 mg. T_g was taken as the inflection point in the heat enthalpy data. Melting endotherms were also identifiable.

RESULTS

IR spectra of an organic compound are generally very rich. In a blend, a majority of the active IR bands due to various components overlap. Therefore, identification of individual components from an IR spectra is difficult, particularly if one is interested in a quantitative measure of a component of the blend. To do so, one must either find an isolated IR band which is associated with the component of interest or, in case bands overlap, develop a deconvolution procedure to identify the intensity profile of that band. It is also possible to isolate IR spectra of a component in a blend from a difference spectra provided that an internal standard for normalization is available. In

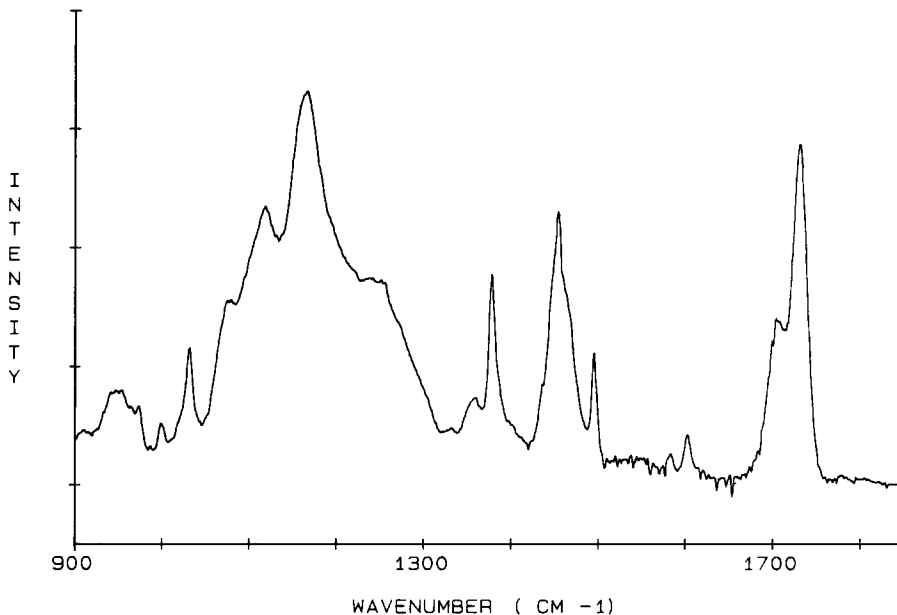


Fig. 1. ATR spectra of a typical blend composition.

our analysis, we have used the difference spectra and the deconvolution procedure to measure relative amounts of the components present in the blends of this study. Each of these methods has its share of uncertainties and one must exert good judgment in using these procedures.

An ATR spectrum of a typical blend composition of this study is shown in Figure 1. ATR spectra of the individual blend components and a blend were used to identify IR bands that were used to determine concentration of the three components in a blend film. We will discuss in detail the methods used for identification of the components in later sections.

The IR band with intensity maximum at 1734 cm^{-1} is assigned to the —C=O stretch mode of the ester group in polymer A.¹⁰ The band with intensity peak at 1703 cm^{-1} is associated with the —C=O stretching mode of the acrylic acid group in polymer B and the methacrylic acid in polymer A.¹⁰ A ratio of the intensities of these two bands (area under the band) using simple mathematical manipulation gives the relative ratio of polymers A to B in volume of the film sampled by the IR beam.

The analysis described is based on the assumption that the carbonyl stretch mode for the acid groups occurs at 1703 cm^{-1} only. It has been shown that a fraction of the acid groups (depending on copolymer structure and film morphology) also contribute to a band at 1730 cm^{-1} due to the nonbonded carboxylate carbonyl stretch mode.^{10,11} In our preliminary analysis, polymer B showed only a small contribution to 1730 cm^{-1} band. Furthermore, it can be shown that neglecting the nonbonded carboxylate contribution only affects the absolute value of the acrylate to acid ratio. Any difference between the ratio for various incidence angles (for various depths of penetration by IR beam), if present, is still valid.

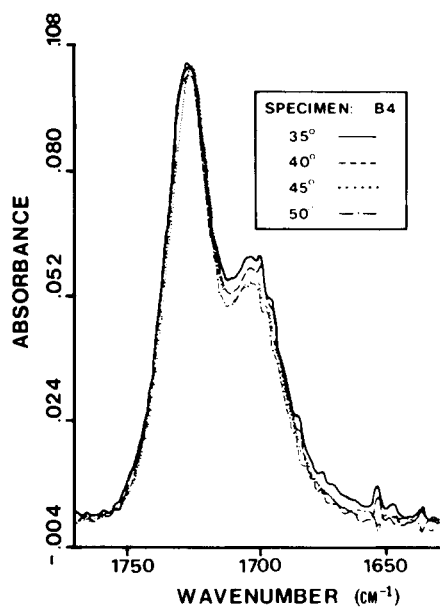


Fig. 2. ATR spectra of the blend composition B4. Incidence angles are: (—) 35°; (---) 40°; (···) 45°; (-·-) 50°.

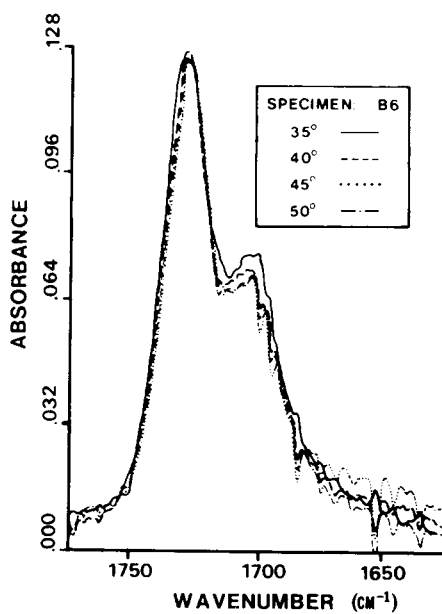


Fig. 3. ATR spectra of the blend composition of B6. Incidence angles are: (—) 35°; (---) 40°; (···) 45°; (-·-) 50°.

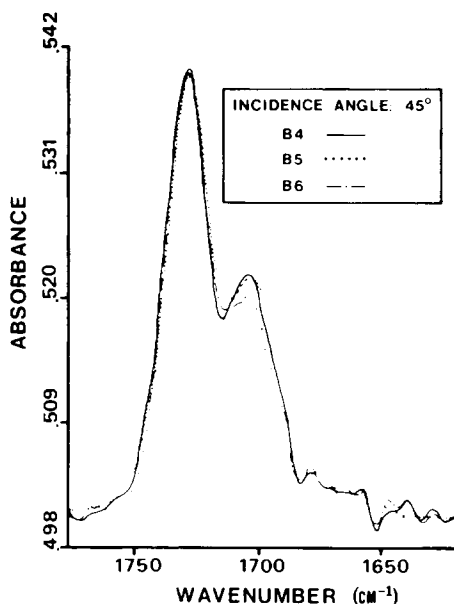


Fig. 4. ATR spectra for incidence angle of 45° for blend compositions: (—) B4; (···) B5; (---) B6.

Two methods used to compare the concentrations of the polymers A to B are described below.

Figures 2 and 3 show results of comparison for a sample at various incidence angles. These plots are obtained by numerically adjusting the peak intensity of the 1734 cm^{-1} band to be the same for all incidence angles, i.e., we use the acrylate band to normalize the spectra for comparison (an assumption is made that the peak intensity at 1734 cm^{-1} is not affected by tail of the 1703 cm^{-1} band). At constant acrylate peak intensity, the peak intensity of 1703 cm^{-1} band, due to acrylic acid in polymer B, decreases slightly with increased angle of incidence. Such change in relative ratio of peak intensity for polymer B to polymer A with incidence angle is consistently observed for all blend specimens. We will describe the results of a second method of analysis which employs a deconvolution procedure in a later section.

In Figures 4 and 5, we show the spectra normalized in the manner described above, for blend specimens of various compositions for a fixed incidence angle. The results show that for a given incidence angle the ratio of polymer B to polymer A is the same for various blend specimens. This is to be expected since the relative amount of polymer B to polymer A was kept constant in preparation of all blend specimens. These results demonstrate that presence of a third component, polymer C, has no effect on the relative distribution of polymers A and B through the film thickness.

Differences in the intensity among various specimens in Figures 4 and 5 are also representative of the experimental scatter (error) in the data. A comparison with the results in Figures 2 and 3 clearly shows that the differences reported earlier for a given specimen at various incidence angles (Figs. 2 and 3) are real and not due to experimental error in the measurements.

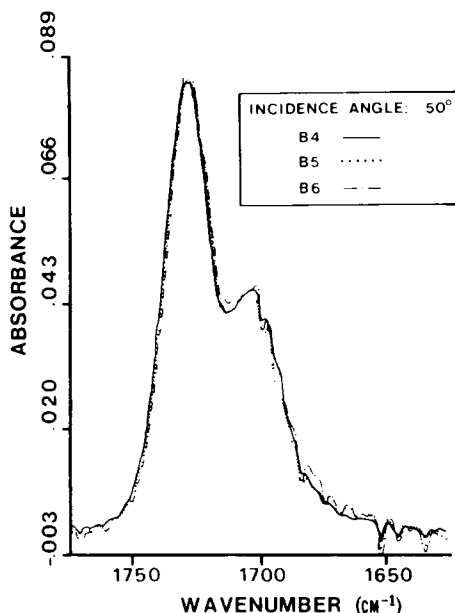


Fig. 5. ATR spectra for incidence angle of 50° for blend compositions: (—) B4; (···) B5; (---) B6.

Only a qualitative interpretation of the relative concentration of polymer A to polymer B is possible from the results in Figures 2 and 3. A quantitative determination of the two polymers can be made if a deconvolution is carried out. Deconvolution program which allows least square fit of a given spectral profile to assumed mathematical functions for the line shapes was used to analyze the spectral region of the 1650–1760 cm^{-1} wavenumber in Figures 2 and 3.

Two IR active modes with intensity peaks at 1703 and 1732 cm^{-1} , due to polymers B and A, respectively, were assigned to represent the overall intensity profile. Gaussian and Lorentzian band shapes were chosen to represent the 1732 and 1703 cm^{-1} band intensity profiles, respectively. The reasons for this choice are explained in the Appendix. The results of deconvolution are shown in Figures 6 and 7 for some of the specimens. Also shown are the deconvoluted intensity profile of the individual bands and an estimated overall intensity profile along with the experimental data. The last two match extremely well throughout the entire wavenumber region.

In Table II, we have compiled the ratio of intensity of the bands due to polymer A and polymer B, determined from the area under the deconvoluted curves. These results show that the ratio of intensity of polymer A to polymer B varies through the film thickness. We will discuss these results in a later section.

Polymer C distribution through the film thickness was also analyzed. A deconvolution procedure similar to that discussed above could not be used since appropriate bands are not available. A spectrum due to polymer C was obtained for each incidence angle by subtracting a normalized spectrum of the blend film without the polymer C from that with the polymer C. The internal

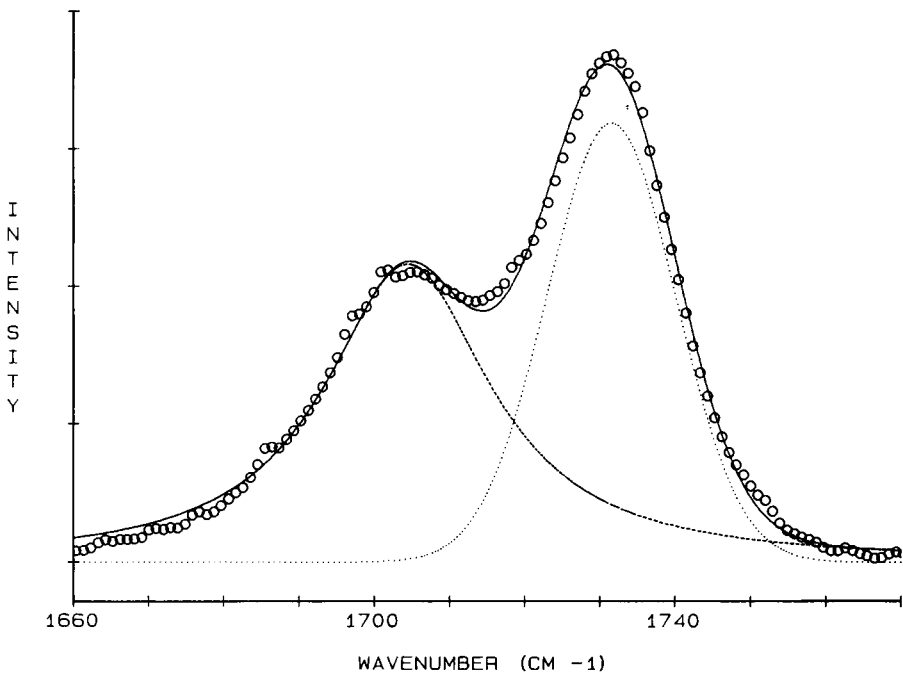


Fig. 6(a). Blend spectra for specimen B4 at incidence angle of 40° ; (\circ) experimental; (---) deconvoluted 1703 cm^{-1} band; (\cdots) deconvoluted 1732 cm^{-1} band; (—) sum of deconvoluted bands.

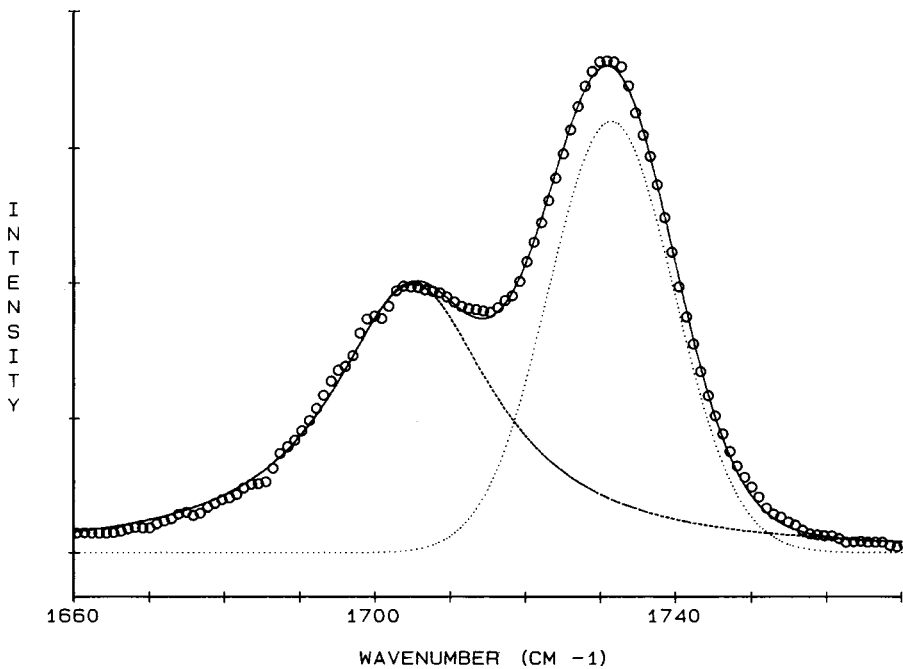


Fig. 6(b). Blend spectra for specimen B4 at incidence angle of 50° ; (\circ) experimental; (---) deconvoluted 1703 cm^{-1} band; (\cdots) deconvoluted 1732 cm^{-1} band; (—) sum of deconvoluted bands.

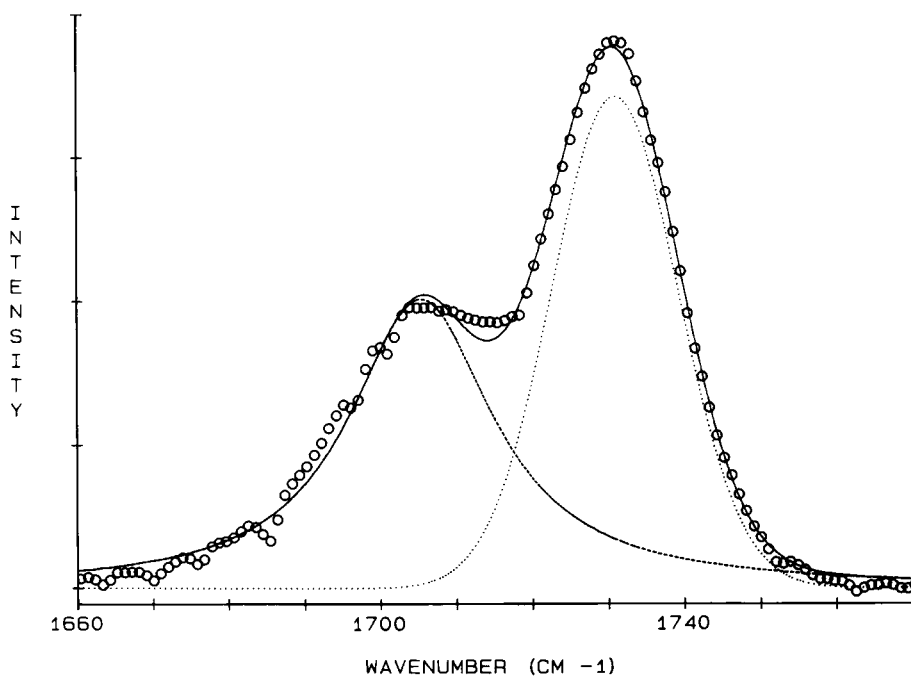


Fig. 7(a). Blend spectra for specimen B6 at incidence angle of 40° ; (O) experimental; (---) deconvoluted 1703 cm^{-1} band; (\cdots) deconvoluted 1732 cm^{-1} band; (—) sum of deconvoluted bands.

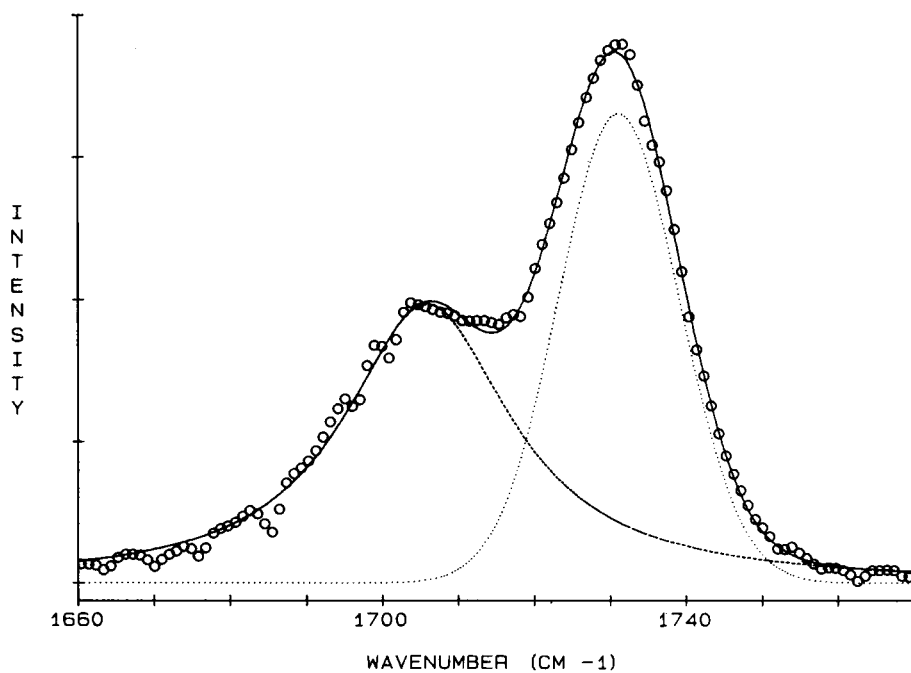


Fig. 7(b). Blend spectra for specimen B6 at incidence angle of 50° ; (O) experimental; (---) deconvoluted 1703 cm^{-1} band; (\cdots) deconvoluted 1732 cm^{-1} band; (—) sum of deconvoluted bands.

TABLE II
Comparison of Relative Amounts of Polymer A to Polymer B
for Various Incidence Angles

Specimen	Incidence angle (deg)	Intensity ratio:
		Acrylic band at 1732 cm ⁻¹ Acid band at 1703 cm ⁻¹
B1	35	0.85
	45	1.10
B3	35	0.80
	45	1.05
B4	35	0.85
	40	0.90
	45	1.00
B5	50	1.05
	35	0.70
	40	0.95
B6	45	1.15
	35	0.85
	40	1.05
	50	0.95

standard used for intensity normalization is the 700 cm⁻¹ styrene band due to monosubstituted benzene ring in polymers A and B.¹⁰ The intensity of this band, i.e., the combined contribution from polymers A and B, was used for normalization.

In Figure 8, we show the difference spectra in a selected wavenumber region for the blend specimen B6 for incidence angles of 35° and 50°. IR bands show higher intensity of the polymer C in the film layers close to the surface which is open to the air. Signal-to-noise ratio of the difference spectra is very poor. Therefore, analysis of the blend films with low concentration of polymer C is not reliable. This result will be discussed further in the discussion section.

THERMAL ANALYSIS

Heat enthalpy curves for dry films of polymers A, B, C, and a representative blend are shown in Figure 9. Heat enthalpy curves for the blend show a melting endotherm which is associated with the polymer C. Based on this observation, we conclude that the crystalline domains of the polymer C are phase-separated. In theory, a comparison of the heat enthalpy curves of the blend with that of the polymers A and B would allow one to determine whether two polymers form a homogeneous system or are phase-separated. However, the glass transition temperatures of the polymers A and B are very close and the blend shows a continuous change in the heat enthalpy in the region of the glass transition temperatures of polymers A and B. As a result, one cannot make any conclusions regarding the phase nature of the polymers A and B based on heat enthalpy data alone. However, studies on closely related systems show that these polymers phase separate.¹² These studies also indicate that the polymer B forms a continuous phase at concentration of approximately 25% or above. Furthermore, the study hypothesizes that the

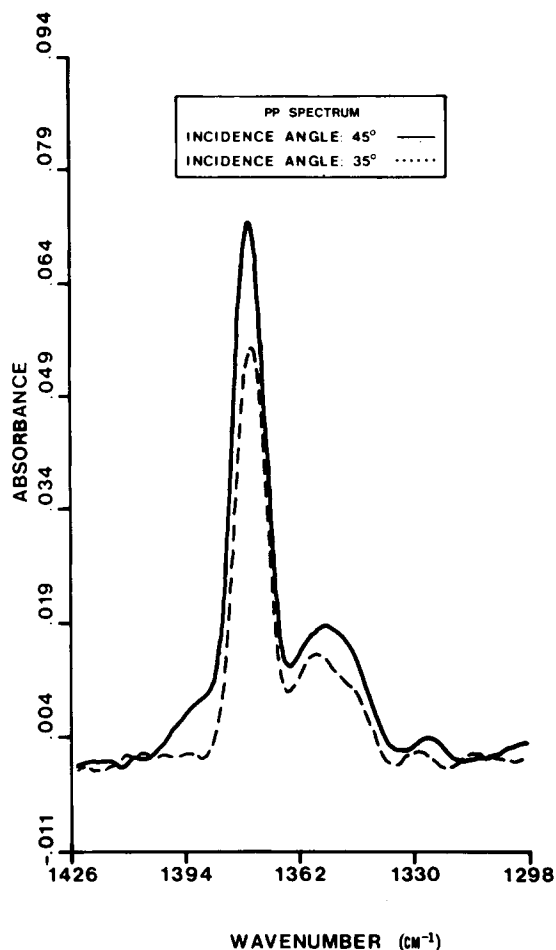


Fig. 8(a). Comparison of normalized spectra of PP for 1377 cm^{-1} band at incidence angles of (\cdots) 35° and (—) 45° .

polymer analogous to polymer A is distributed as particles inside a matrix formed by a polymer similar to the polymer B.¹² Polymer B concentration in our study varies from 37% to 24% as concentration of the polymer C increases. Therefore, we expect that the polymers A and B are also phase-separated in the blends of this study.

Thin films of the blend specimens are clear. Thick film specimens (~ 0.5 mm) show no haze for the blend of polymers A and B alone. Haze increases as concentration of the polymer C in the specimen is increased. At polymer C concentration near 70%, haze in the film disappears. These observations confirm that the polymer C, when present in low concentration, is phase-separated.

Our aim here is to point out that we are working with a phase-separated system. A detailed investigation of the morphological aspects and its effects on properties of the blends is continuing.

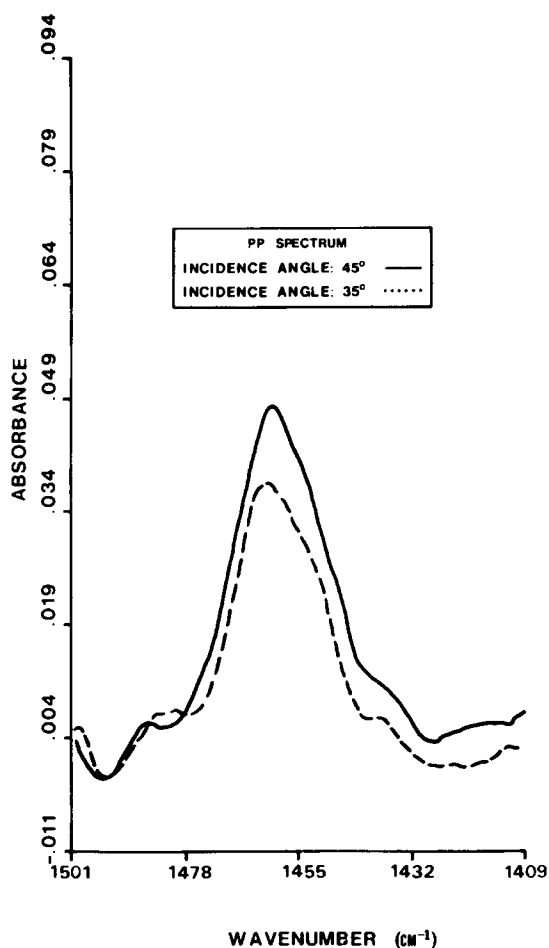


Fig. 8(b). Comparison of normalized spectra of PP for 1461 cm^{-1} band at incidence angles of (\cdots) 35° and (—) 45° .

DISCUSSION

Two main requirements for a good quality (i.e., relatively high signal-to-noise ratio) and undistorted ATR spectra are: (a) a good contact between the sample and the ATR crystal and (b) incidence angles far above the critical angle. Critical angle θ_c is defined as where $\theta_c = \sin^{-1} n_2/n_1$, where n_2 and n_1 are the refractive indices of the sample and the crystal, respectively. Spectra obtained at incidence angle close to the critical angle will show distortions in the band shapes. Poor contact between the crystal and the sample results in a noisy spectra. Another reason for the poor signal-to-noise ratio in an ATR spectra is the small beam penetration of $0.3\text{--}1\ \mu\text{m}$ in a typical reflection in the ATR mode. Accounting for the 10–12 reflection along the length of an ATR crystal, the total volume of the specimen monitored in ATR mode is equivalent to a specimen $3\text{--}10\ \mu\text{m}$ in thickness. This sample thickness is generally much smaller than the films examined in transmission. The beam penetration depth into the specimen also varies with the wavenumber of the band, since

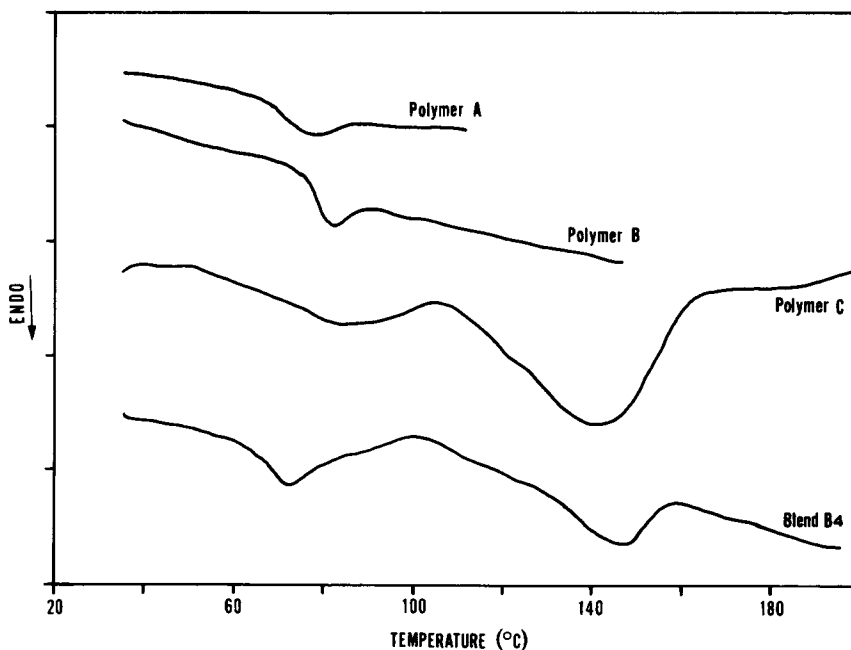


Fig. 9. Heat enthalpy curves: (a) polymer A; (b) polymer B; (c) polymer C; (d) blend B4.

the specimen refractive index depends on the wavelength of the light. Furthermore, multiple reflections at the crystal/specimen boundary cause scattering of light, an additional source of noise not present in the transmission mode. These are some of the reasons why quantitative interpretations of the ATR data are difficult and such studies in the literature are scant.

In our studies, signal-to-noise ratio was improved by placing two pieces of the specimen film, one on each side of the crystal. This increases the signal by a factor of 2. In order to examine the incidence angles used relative to the critical angle, a refractive index of 1.3 for the specimen (n_2) was assumed. This value is quite reasonable, since measured values of the refractive indices for most of the coatings are generally 1.25–1.35. The refractive index for germanium is 4.0. This gives a critical angle of approximately 19° . Our experimental measurements were made at incidence angles of 35° and above, which is far above the critical limit. Therefore, the spectra obtained should be free of distortions and one is confident of using the band shape and intensity data for quantitative analysis.

The data shown in Table II, being a ratio, are dimensionless. The numbers in the column labeled "intensity ratio" are valid only for comparison. In other words, a ratio of 1.0 in Table II does not imply equal amounts of resin and emulsion polymer in the blend but solely that the areas of the two bands are the same. In order to convert these numbers to relative amounts of the two polymers, one needs to know the absorption coefficients for the two bands and beam penetration depth of the specimen at the wavelength of the absorption bands. The beam penetration depth, in particular, cannot be obtained precisely. Therefore, no attempt is made to convert the band area ratio to a ratio of the amounts of two polymers present.

A comparison of the results in Table II, for any blend specimen at different incidence angles shows that a concentration gradient of the polymers A and B exists through the film thickness. The data in Figures 2 and 3 also show similar effects but the changes appear to be much smaller. This is precisely the reason that in a previous communication, i.e., when deconvolution procedure was not used, we reported that polymers A and B are uniformly distributed through the film thickness.^{13,14} Furthermore, earlier reports were based on the data obtained using KRS-5 crystal, where the incidence angles were much closer to the critical angle, due to lower refractive index of the KRS-5 crystals. This caused severe band distortions, and data interpretation required additional assumptions to correct for the band distortions. Therefore, improved precision using germanium crystal also allows us to detect smaller concentration differences than was possible with KRS-5.

An alternate explanation of the observed differences between the germanium and KRS-5 crystals is as follows. The estimated depth of penetration using the germanium crystal, as mentioned earlier, is 0.30–0.55 μm for the incidence angles used. The depth of penetration for experiments using the KRS-5 crystal is estimated at 0.85–1.20 μm , which is greater by a factor of approximately 2.5 over that for germanium.¹³ Supposing that the relative concentration of polymer A to polymer B is constant in the bulk of the film (i.e., at certain distance away from the film surface), it is possible that a gradient in relative concentration exists near the film surface (as is determined using germanium crystal), however farther inside the specimen (from the film surface) the difference in relative concentration with distance is small and not detected (as was seen using KRS-5 crystal). Rutherford backscattering may be used to resolve this issue and experiments are planned to do so.¹⁵

The presence of a gradient in polymer C concentration through the film thickness is shown by the results in Figures 8(a) and 8(b), where normalized bands due to polymer C show change in intensity for various incidence angles. These experimental results indicate a higher polymer C concentration near the film surface. Similar observations of a gradient in polymer C concentration through the film thickness were made using the KRS-5 crystal.^{13,14} The signal-to-noise ratio is poorer with the germanium crystal due to shallower penetration depth of the evanescent IR beam. Therefore, we are able to make reliable measurements using the germanium crystal, only at high polymer C concentration. The KRS-5 crystal, however, allowed measurements at various polymer C concentrations and similar trends were observed in all cases.

In summary, three polymers are not distributed uniformly through the film thickness. The relative ratio of polymer A to polymer B is not uniform at least to a distance of 0.5 μm from the film surface; whether this nonuniformity in polymer A to polymer B ratio extends farther to a distance of 1.2 μm or so cannot be answered due to uncertainty in measurement of concentration ratio using KRS-5 crystal. However, the results from KRS-5 and germanium crystals both show that polymer C concentration decreases as one moves farther inside from the film surface. Therefore, polymer C concentration gradient extends at least up to a distance of 1.2 μm from the film surface.

Why does a concentration gradient of components in a blend film occur? It is not a result of density differences between components, at least for the case of the polymers A and B, because density of the polymer A is greater than that of the polymer B (1.075 ± 0.015 to 1.055 ± 0.015 g/mL, respectively). If

a concentration gradient through the film thickness was due to sedimentation effects during the time of film drying, one would expect a higher concentration of the polymer B near the film surface which is opposite to that observed experimentally. Therefore, these effects must arise due to surface energy considerations. However, density of the polymer C is 0.870 ± 0.020 g/mL. As a result, density differences must partially contribute to the observed concentration differences through the film thickness, although surface energy effects are likely to contribute as well.

Thermal behavior of the blends clearly shows that various components are phase-segregated in the bulk of the blend film. No direct information on the phase behavior near the film surface is available. However, the size, shape, and orientation of various component phases, near the film surface, can possibly influence the observed relative intensity ratios using ATR. More work to investigate the near surface morphology of the films is needed. Nevertheless, the compositional differences near the film surface relative to the bulk are important in understanding the near-surface properties of the polymer blend films.

In conclusion, dry films from a multicomponent blend show nonuniform composition through the film thickness. Near surface composition and by association properties of the films are different from the interior bulk. These observations are important since many useful properties of the blend films such as gloss, wear resistance, friction coefficient, etc., must relate strongly to the film composition near the surface.

APPENDIX

The deconvolution procedure was carried out using a least-square fit of the experimental data to the assigned band profiles for the acid and the ester bands. The choice of a Gaussian band shape for the —C=O stretch of the ester is based on the best fit obtained for this band for the ester group in PMMA (see Fig. 10). No significant improvement in the data fit is achieved by allowing a combination of the Gaussian and Lorentzian bands.

The second band in the deconvoluted spectra is due to the —C=O stretch of the bonded acid groups at approximately 1703 cm^{-1} . With an assigned Gaussian profile for the ester IR band, a Lorentzian band profile for the 1703 cm^{-1} band gives the best least-square fit of the experimental data. Therefore, the Gaussian and Lorentzian profiles for the 1732 and 1703 cm^{-1} bands, respectively, were used for deconvolution.

In addition, a least-square fit of the experimental data for a blend specimen was attempted, allowing each band to assume a combination of the Gaussian and Lorentzian band profiles. The fit showed less than 5% contribution from the Gaussian mode to the 1703 cm^{-1} and of the Lorentzian to the 1732 cm^{-1} bands, respectively. This again demonstrated that choice of the band shapes mentioned in the previous paragraph were appropriate for deconvolution.

The authors appreciate the help of Dr. C. Weiss with deconvolution of the spectra. The authors would also like to thank Drs. J. M. Pochan and J. R. Allaway and Ms. D. T. Krawczak for many valuable suggestions. The support of this work by Drs. D. J. Grosse and P. J. Conigliaro is also

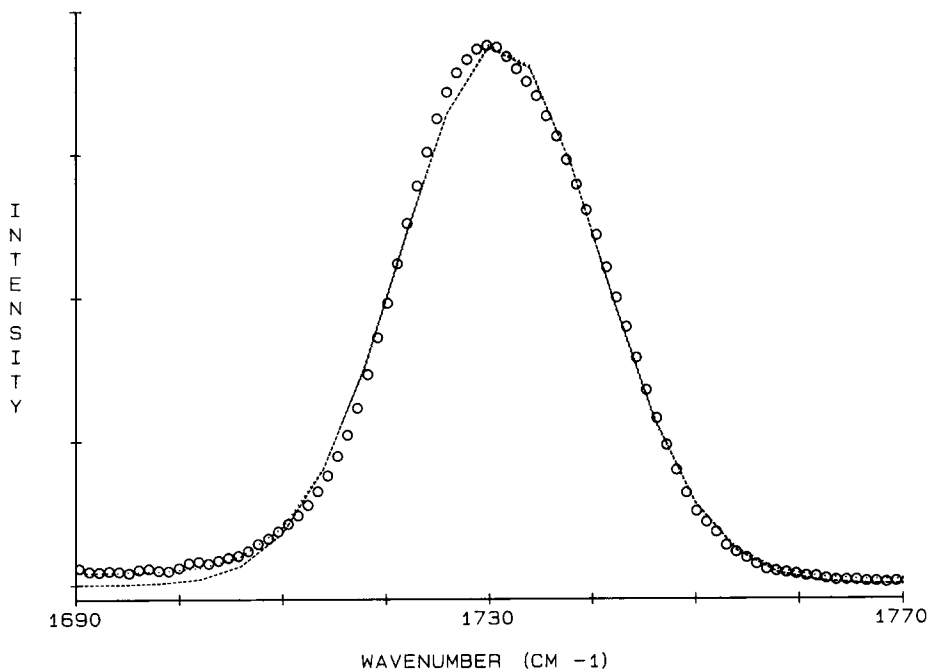


Fig. 10. PMMA spectra for incidence angle of 45° and fit according to GAUS-LOR; (\circ) experimental; (---) Gaussian; (\cdots) Gaussian plus Lorentzian.

acknowledged. Finally, it is a pleasure to acknowledge the assistance of Ms. Sandra Determan in typing this report.

References

1. P. A. Wilks and T. Hirschfeld, *Appl. Spectrosc. Rev.*, **1**, 99 (1967).
2. N. J. Harrick, *J. Opt. Soc.*, **55**, 851 (1965).
3. P. Blais, D. J. Carlsson, G. W. Csullog, and D. M. Wiles, *J. Colloid Interface Sci.*, **47**, 636 (1974).
4. W. T. M. Johnson, *Off. Digest Oil Colour Chem. Assoc.*, **32**, 1067 (1960).
5. H. A. Willis and V. J. I. Zichy, *Polymer Surfaces*, D. T. Clark and W. J. Feast, Eds., Wiley, 1978, pp. 287-307.
6. T. Hirschfeld, *Appl. Spectrosc.*, **31**, 289 (1977).
7. J. L. Koenig, L. D'Esposito, and M. K. Antoon, *Appl. Spectrosc.*, **31**, 292 (1977).
8. F. M. Mirabella, *J. Polym. Sci., Polym. Phys. Ed.*, **23**, 861 (1985).
9. F. M. Mirabella, *J. Polym. Sci., Polym. Phys. Ed.*, **20**, 2309 (1982).
10. *Aldrich Library of Infrared Spectra*, 2nd ed., Charles J. Pouchert, Ed., Aldrich Chemical Company, Milwaukee, 1975.
11. J. R. Allaway, private communication, S. C. Johnson and Son, Inc.
12. K. M. O'Connor and E. B. Orler, *Proc. 14th Water Borne and Higher Solids Coatings Symp.*, New Orleans, LA, 1987, p. 143.
13. R. Popli and A. M. Dwivedi, *Int. Conf. on Fourier and Computerized Infrared Spectroscopy*, SPIE **553**, 1985, p. 120.
14. A. M. Dwivedi and R. Popli, *ATR Studies of Polymer Blend Films*, SCJ Corporate Research Reports, 1985 and 1986.
15. J. F. Romanelli, J. W. Mayer, and E. J. Kramer, *J. Polym. Sci., Polym. Phys. Ed.*, **24**, 263 (1986).

Received November 23, 1987

Accepted July 8, 1988